16th World Conference on Earthquake, 16WCEE 2017
Santiago Chile, January 9th to 13th 2017
Paper N° 970 (Abstract ID)
Registration Code: S-C1463173743

IMPLICATIONS OF FRICTION COEFFICIENT VARIATION IN THE SEISMIC ANALYSIS OF STRUCTURES WITH TRIPLE FRICTION PENDULUM SYSTEMS (FPT). AN APPLICATION CASE

R. Aguiar (1), G. Villarruel (2), P. Caiza (3)

(1) Research and Teaching
Roberto Aguiar Falconí (Main Autor)
Universidad de las Fuerzas Armadas -ESPE.
Departamento de Ciencias de la Tierra y la Construcción, Facultad, Ingeniería Civil
Av. Gral. Rumiñahui s/n. Valle de los Chillos, Ecuador.
rraguiar@espe.edu.ec

(2) Undergraduate
Gissela Villarruel Flores
Universidad de las Fuerzas Armadas -ESPE.
Departamento de Ciencias de la Tierra y la Construcción, Facultad, Ingeniería Civil
gevillarruel@espe.edu.ec

(3) Research and Teaching
Pablo Enrique Caiza Sánchez
Universidad de las Fuerzas Armadas -ESPE.
Departamento de Ciencias de la Tierra y la Construcción, Facultad, Ingeniería Civil
Av. Gral. Rumiñahui s/n. Valle de los Chillos, Ecuador.
pecaiza1@espe.edu.ec

Abstract

The earthquake at Pedernales in April 16 2016, of magnitude 7.8, caused too much damage in the structures of the provinces of Manabi and Esmeraldas in Ecuador, and marked the beginning of a new way of construction using passive control systems, such as seismic isolators or energy dissipators.

At Universidad de las Fuerzas Armadas ESPE, located in the Valley of Los Chillos in Ecuador, five structural blocks with triple friction pendulum seismic isolators are being built.

This paper describes the results of tests conducted to 61 isolators of this construction project, subjected to vertical loads of 250 tonf. In each test, three load cycles were applied at a rate of 12 seconds each, with a maximum amplitude of 30 cm. The friction coefficients obtained in each cycle and in each isolator were recorded. On this basis, three sets of data for the coefficient of friction of the plates of the isolation system were selected: one data base with maximum values, other with minimum values and another with nominal values.

With these values, a seismic analysis was performed on the ESPE structural blocks using the simplified analysis model in ASCE 7, the Mc Vitty and Constantinou (2015) three-stages model and the Fenz and Constantinou (2007) five-stages model. The results are compared in terms of displacements and forces.

Finally, the force and displacement results were compared at each level of friction coefficients: maximum, minimum and nominal values.

Keywords: Triple friction pendulum seismic systems (FPT), Maximum value of frictional coefficient, Minimum value of frictional coefficient and Nominal value of frictional coefficient.

1. INTRODUCCIÓN

At the Universidad de las Fuerzas Armadas ESPE, located in the Valley of Los Chillos in Ecuador, five steel framed building blocks with seismic triple friction pendulum isolators are being built. The isolator used is of the type FTP8833 / 12-12 / 8-6, shown in Figure 1. (Constantinou *et al.* 2016; Aguiar *et al* 2016).

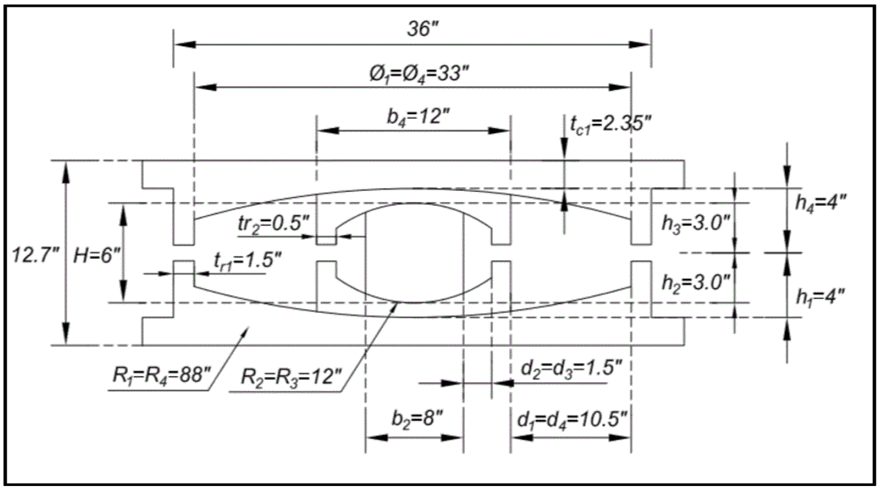

Fig. 1 - Geometry of the triple friction pendulum isolator FTP8833 / 12-12 / 8-6
Source: Constantinou *et al.* 2016; Aguiar *et al* 2016).

Figure 2 shows the structural blocks being built at Universidad de las Fuerzas Armadas ESPE. In the structural blocks 1 and 8, the isolators are placed on pedestals just above the concrete footings. At blocks 2 and 3, which have an underground story, the isolators are placed on top of reinforced concrete columns. Finally, at structural block 6-7 a mix of the previous solutions was employed.

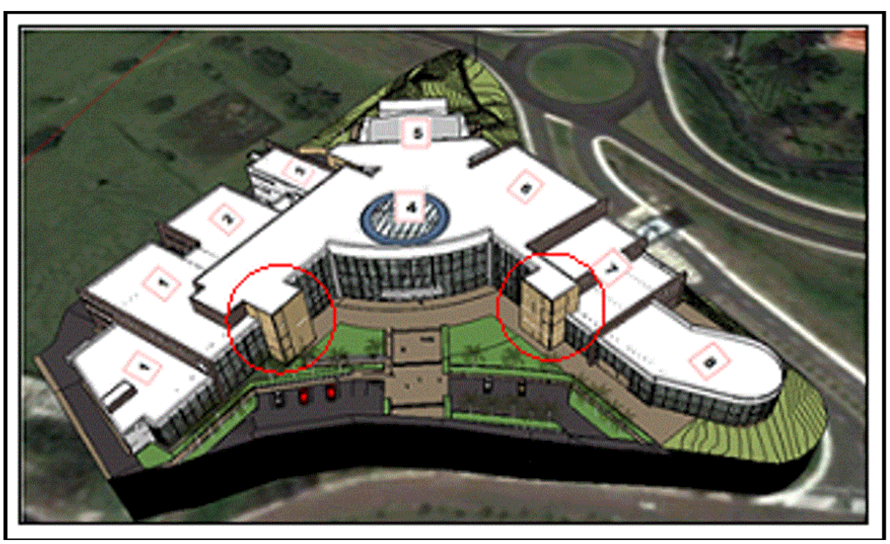

Fig. 2 - Overview of the Structural Blocks at Universidad de las Fuerzas Armadas ESPE

Details of these solutions are presented in Fig.3. To the left, the isolation system on top of the column is shown. Observe that a 120/120 cm concrete basket allows that the isolator is fully supported at its base. To the right of Figure 3 the other type of isolator, on top of a pedestal, is also shown.

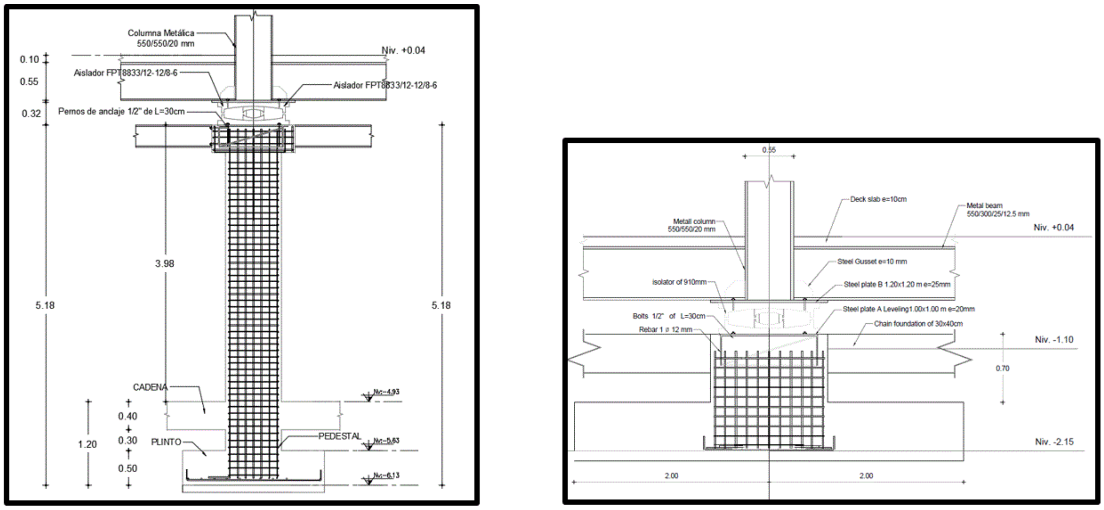

Fig. 3 – FPT isolator on top of column and on top of pedestal. Source: Aguiar and Pazmiño (2016)

This paper describes the structural seismic analysis of the structural block 3. Three constitutive models for the isolators are considered. They are described in the next paragraphs. They are the linear model of ASCE 7-10, the 5-stages model of Fenz and Constantinou (2007, 2008) and the three-stages model proposed by Mc Vitty and Constantinou (2015).

The coefficients of friction are experimentally obtained in 61 isolators with a vertical load of 250 tonf (EPS, 2015). Maximum, nominal and minimum values are applied to the 3-stages, 5-stages and the simplified linear method of the ASCE 7-10 and analyzed using the spectral method (Aguiar, 2012).

2. CONSTITUTIVE MODEL

Using the simplified linear model of ASCE 7-10, the effective stiffness of the isolators k_{ef}, the damping factor ξ_{ef}, the vibration period of the isolated structure T , and the displacements and forces in the center of mass (CM) were found. In contrast, in the 3-stages and 5-stages models only k_{ef} y ξ_{ef} were determined. The isolator was modeled as a short element (Almazan, 2001; Fenz y Constantinou *et al*., 2006).

2.1 ASCE 7-10 Model

Figure 4 shows the constitutive model that ASCE 7-10 considers to define the behavior of a FPT isolator. Based on this model, the following parameters are determined:

$$k_{ef} = \frac{W}{R} + \frac{\mu W}{D} \tag{1}$$

$$\xi_{ef} = \frac{2}{\pi}\left[\frac{\mu}{\mu + \frac{D}{R}}\right] \tag{2}$$

$$\mu W = \left[\mu_1 - (\mu_1 - \mu_2)\ \frac{R_{2ef}}{R_{1ef}}\right] W \tag{3}$$

$$R_{ief} = R_i - h_i \qquad \longrightarrow i = 1,2,3,4 \tag{4}$$

Where μ_1, μ_4 are the friction coefficients of the plates with radius R_1, R_4 (outside radius), μ_2, μ_3 are the coefficients of friction of the inner plates of radius R_2, R_3 (see Figure 1), h_i , for i = 1,2,3,4, is the height of the isolator defined in Figure 1, μ is the equivalent coefficient of friction, W is the total weight on the isolator, D is the expected lateral displacement in the isolator, R is the radius of curvature of the isolator equal to the sum of $R_{1ef} + R_{2ef}$. (Constantinou, M. C, Whittaker, A. S., Kalpakidis, Y., Fenz, D. M. and Warn G. P. 2007).

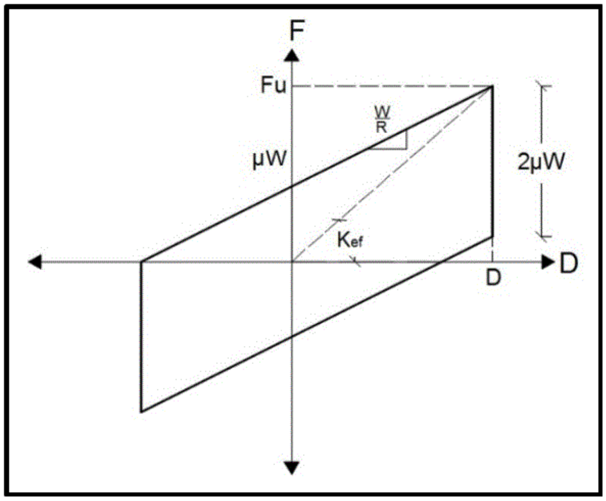

Fig. 4 - Bilineal constitutive model for the FPT isolator. Source: Mc Vitty y Constantinou (2015)

On the other hand, the period T and the displacement D of a system of one degree of freedom are calculated using the following equations:

$$T = 2\pi \sqrt{\frac{W}{k_{ef}\, g}} \tag{5}$$

$$D = \left(\frac{S_1 * g}{4\,\pi^2}\right) \frac{T}{B} \tag{6}$$

Additional variables are g as the gravity acceleration, S_1 is the coefficient of g found in the elastic design spectrum for a period of 1 second, B is the factor that allows to obtain spectra for any damping value. The recommended values of B by the ASCE 7-10 are shown in Table 1.

Table 1 - B values for damping other than 5%. Source: ASCE 7-10

ξ_{ef} **(%)**	$\leq \mathbf{2}$	5	10	20	30	40	$\geq \mathbf{50}$
B	0.8	1.0	1.2	1.5	1.7	1.9	2.0

The shear force in the isolated system V_b is calculated with the following equations:

$$V_b = \frac{\sum k_{ef}\ D}{R_D} \tag{7}$$

$$V_s = \frac{\sum k_{ef}\ D}{R_S} \tag{8}$$

$$F_x = V_s\ \frac{W_x\, h_x}{\sum_i^n W_i\, h_i} \tag{9}$$

Where R_D, R_S, are the reduction factors for the infra and superstructure forces (this study considered $R_D = 1$; $R_S = 1.4$), F_x, W_x, h_x, are strength, weight and height measured from the base of the structure to the level of any floor respectively.

As indicated above, the effective stiffness is calculated with maximum, nominal and minimum friction coefficients.

2.2 Three-stages model

The three-stages model (Mc Vitty and Constantinou, 2015) applies when the external surface radius are equal, $R_1 = R_4$; as well as the internal surfaces $R_2 = R_3$. Similar simplifications are possible with heights and coefficients of friction. In this case, the geometrical properties are reduced from 12 to 6 and the friction coefficients of 4 to 2. The three phases of the model are indicated below, noting that all variables have been already defined.

In the first phase, displacement occurs only in the plates 2 and 3.

$$0 \leq u \leq u^*$$

$$u^* = 2\,(\mu_1 - \mu_2)\,R_{2,ef} \tag{10}$$

$$F = \frac{W}{2\,R_{2,ef}}\,u + \mu_2\,W \tag{11}$$

To the left of Figure 5, it can be seen the inner-isolator-moving-surfaces 2 and 3; to the right, the corresponding displacement vs. lateral force graph.

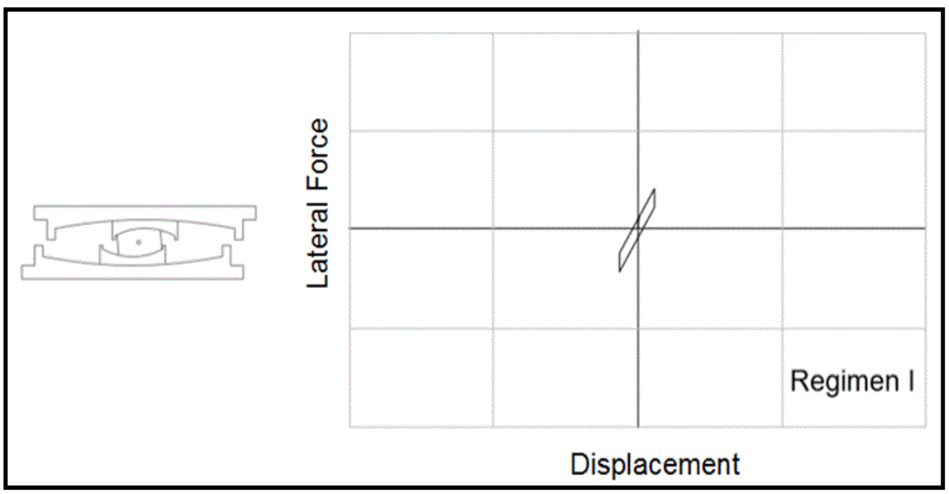

Fig. 5 – Isolator performance in Regime I. Source: Mc Vitty y Constantinou (2015)

In the second phase, the movement in the interior isolator reaches the stops and surfaces 1 and 4 start moving on. Normally, is in this regime that the isolator is working under an earthquake of moderate and high intensity. The equations are shown below and in Figure 6 the corresponding displacement vs. lateral force graph.

$$u^* \leq u \leq u^{**}$$

$$u^{**} = u^* + 2\,d_1^* \tag{12}$$

$$F = \frac{W}{2\,R_{1,eff}}\,(u - u^*) + \mu_1\,W \tag{13}$$

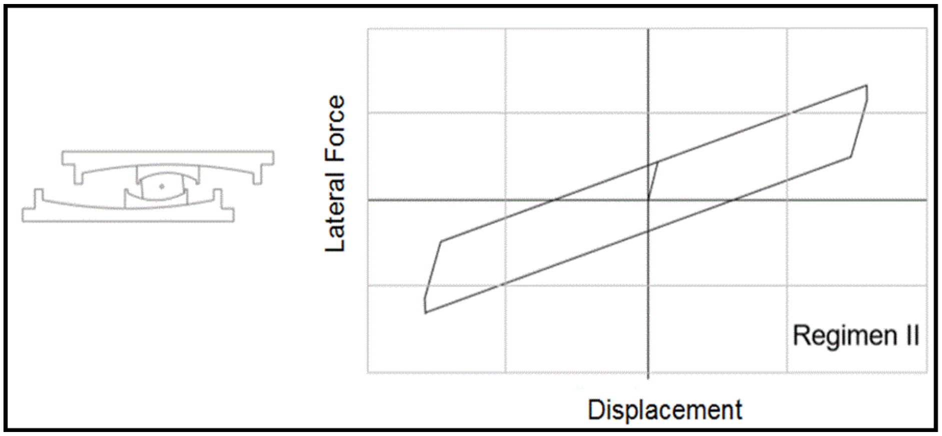

Fig. 6 – Isolator performance in Regime II. Source: Mc Vitty y Constantinou (2015)

The third phase is when the earthquake is extremely strong and the inner isolator meets the outer stops. In these conditions. The inner isolator surfaces 2 and 3 begin to slide, see Figure 7.

$$u^{**} \leq u \leq u_{cap}$$

$$u_{cap} = 2\, d_1^* + 2\, d_2^* \tag{14}$$

$$F = \frac{W}{2\, R_{2,1ff}} (u - u^{**}) + \frac{W}{2\, R_{1eff}} (u^{**} - u^*) + \mu_1 W \tag{15}$$

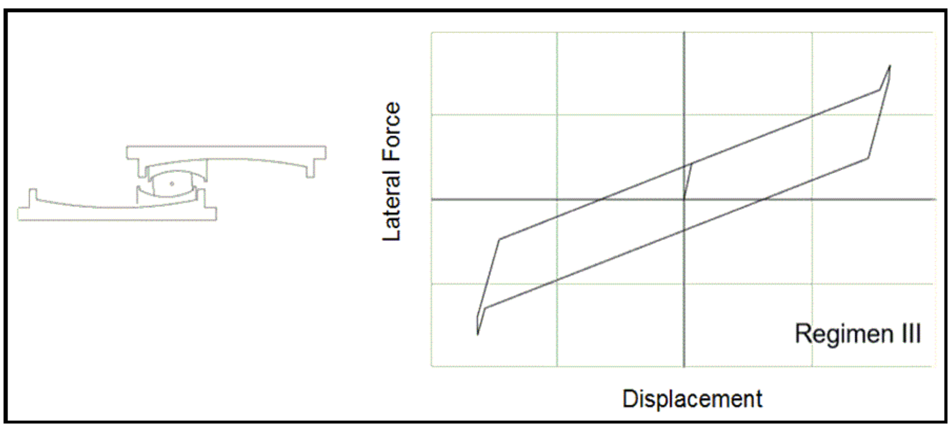

Fig. 7 – Isolator performance in Regime III. Source: Mc Vitty y Constantinou (2015)

2.3 Five-stages model

This model was proposed by Fenz and Constantinou (2007, 2008) and Fadi and Constantinou (2010). It is described below according to the nomenclature shown in Figure 1.

In the first phase, the isolator slides on surfaces 2 and 3; the lateral force F and lateral displacement q are defined by the following equations.

$$0 \leq q \leq q^*$$

$$F = \frac{W}{R_{2,eff}+R_{3,eff}}\, q + \frac{F_{2,f}\, R_{2,eff} + F_{3,f}\, R_{3,eff}}{R_{2,eff}+R_{3,eff}} \tag{16}$$

$$q^* = (\mu_1 - \mu_2)\, R_{2,eff} + (\mu_1 - \mu_3)\, R_{3,eff} \tag{17}$$

In the second phase, the inner isolator slippage occurs on surfaces 1, 2 and 3, as a second generation isolator in which the bearing is the inner isolator. The lateral force F and displacement q are:

$$q^{*} \leq q \leq q^{**}$$

$$F = \frac{W}{R_{1,eff} + R_{3,eff}} q + \frac{F_{1,f}\left(R_{1,eff} - R_{2,eff}\right) + F_{2,f} R_{2,eff} + F_{3,f} R_{3,eff}}{R_{1,eff} + R_{3,eff}} \tag{19}$$

$$q^{**} = q^{*} + (\mu_4 - \mu_1)\left(R_{1,eff} + R_{3,eff}\right) \tag{18}$$

All variables have already been defined. Figure 8 shows the constitutive curves corresponding to phases I and II.

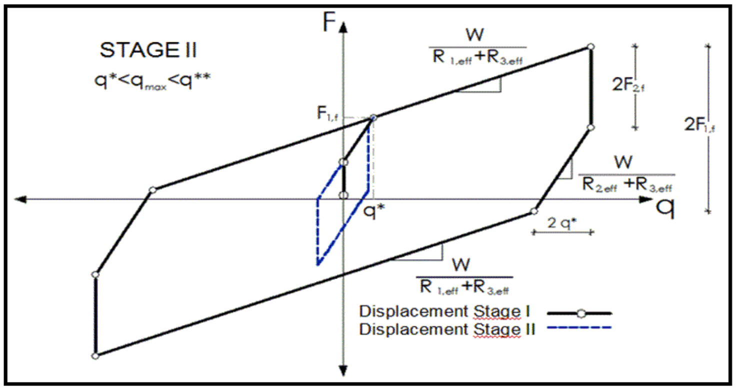

Fig. 8 – Constitutive curves corresponding to stages I and II.
Source: Fenz and Constantinou model (2007, 2008)

The third phase begins when the lateral displacement exceeds q^{**} and starts at F_{4f}. In this regime all four surfaces are sliding. Figure 9 shows the constitutive curve in stage III. The equations that define force and displacement are:

$$q^{**} \leq q \leq q_{dr1}$$

$$F = \frac{W}{R_{1,eff} + R_{4,eff}} q + \frac{F_{1,f}\left(R_{1,eff} - R_{2,eff}\right) + F_{2,f} R_{2,eff} + F_{3,f} R_{3,eff} + F_{4,f}\left(R_{4,eff} - R_{3,eff}\right)}{R_{1,eff} + R_{4,eff}} \tag{20}$$

$$q_{dr1} = q^{**} + d_1\left(1 + \frac{R_{4,eff}}{R_{1,eff}}\right) - (\mu_4 - \mu_1)\left(R_{1,eff} + R_{4,eff}\right) \tag{21}$$

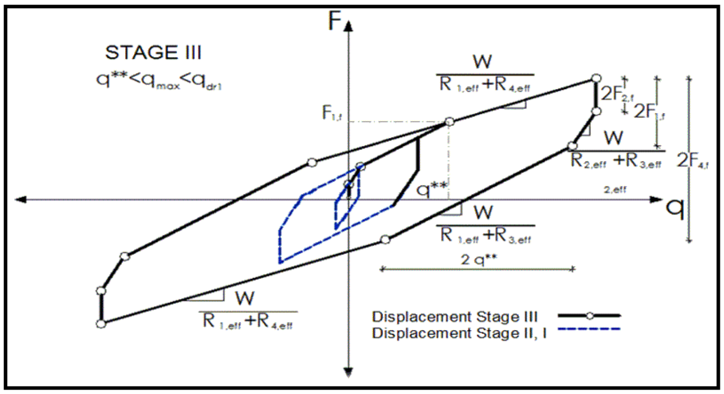

Fig. 9 – Constitutive curve in stage III.
Sourse: Modelo de Fenz y Constantinou (2007, 2008)

In stage IV, the inner isolator reaches one edge and starts with a force $F_{dr1} = \frac{W}{R_{1,eff}} d_1 + F_{1,f}$, associated with a displacement q_{dr1}. The lateral force and displacement are given by the following equations:

$$q_{dr1} \leq q \leq q_{cap}$$

$$F = \frac{W}{R_{2,eff} + R_{4eff}} (q - q_{dr1}) + \frac{W}{R_{1,eff}} d_1 + F_{1,f} \tag{22}$$

$$q_{cap} = 2\, d_1^* + 2\, d_2^* \tag{23}$$

In Figure 10 corresponding to the phase IV curve and previous constitutive presented, until this phase can be considered that the insulator is operable.

Finally, there is a stage V, which is related to the impact of the internal isolator against the stop caps, usually drawn with broken lines to indicate its existence but should not be considered for the structural design.

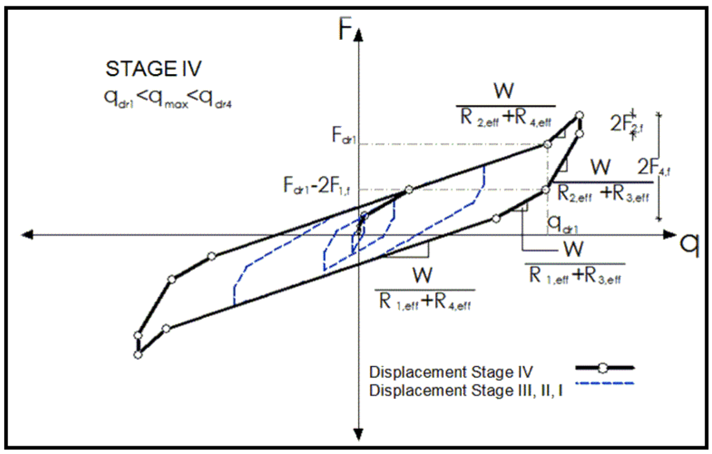

Fig. 10 – Diagrama de histéresis en Fase IV.
Source: Mc Vitty y Constantinou (2015)

3. FRICTION COEFFICIENTS

Sixty-one FTP8833/12-12/8-6 isolators were tested under vertical loads of 250 tonf. Three harmonic cycles with displacement up to 30 cm were applied, in 12 seconds. The results of the friction coefficient are shown in Figure 11, EPS (2015).

Each graph has three curves: maximum, nominal and minimum. These values are shown in Table 2.

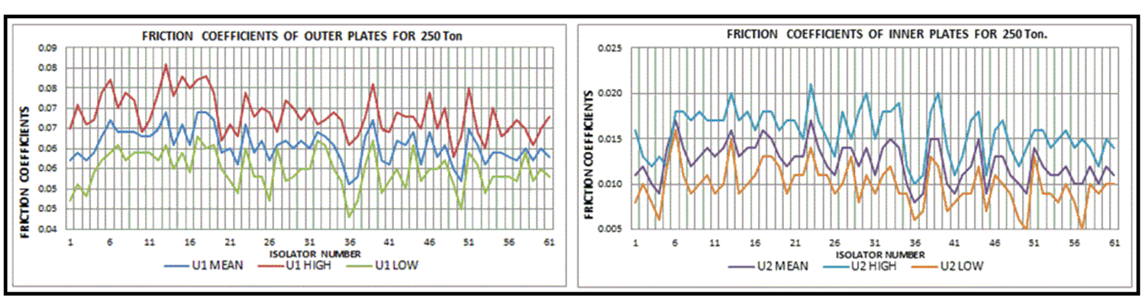

a) b)

Fig. 11 – Friction coefficients for 250 tonf: **a)** Exterior surfaces (μ_1): maximum, nominal and minimum values, **b)** Interior surfaces (μ_2): maximum, nominal and minimum values.

Table 2 - Friction coefficient values used in the structural analysis

FRICTION COEFICIENTS	MAXIMUM	NOMINAL	MINIMUM
μ_1	0,068541	0,060754	0,054738
μ_2	0,015672	0,012426	0,009885

4. STRUCTURE ANALYSIS

The seismic analysis of the Structural Block 3 (See Figure 2), where the isolators are placed on reinforced concrete columns, was performed. The columns are 550/550/20 mm tubular sections and the beams are type I 550/300/25/12 sections. The steel used is the A572, with a yielding stress of 45700 MPa. In Figure 12 a) a 3D view of the structure is presented and in Figure 12 b), the degrees of freedom which were considered.

A model of three degrees of freedom per floor, two horizontal displacements and a rotation of the floor was used. (Aguiar, 2012; Retamales, R., Bonelli, P., Boroschek, R. y Carvallo, J., 2015; Chistopupoulus,C. and Filiatraul, A.,2006).

The structure has 5 stories plus a short element representing the isolators. The spectral method was used for the analysis; with effective stiffness values calculated using the 3- and 5-stage models. The ASCE 7-10 model was worked with the simplified linear method. (Chopra A. K.,2001).

The analysis earthquake is defined by the design spectrum of the Ecuadorian Construction Norm NEC-15, to the Valley of Los Chillos where $z = 0.4$, in a profile type C. The seismic force reduction factor was $R = 1.4$.

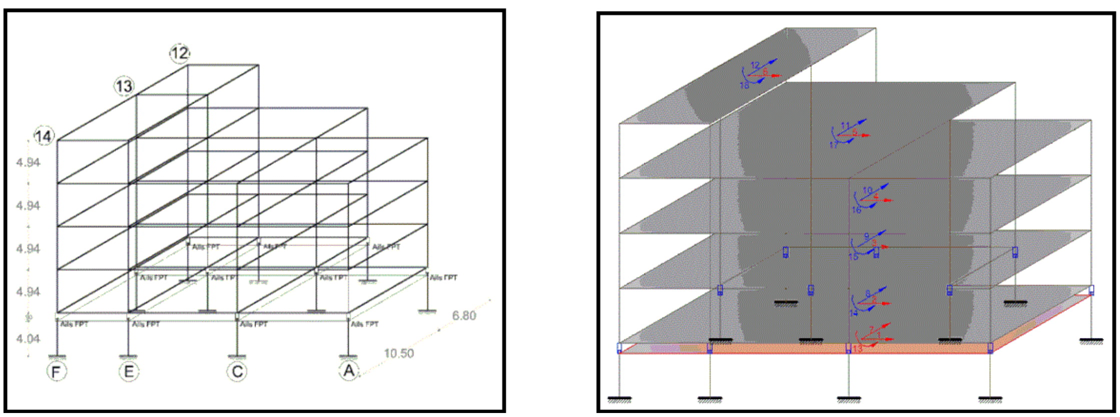

a) **b)**

Fig. 12 – Structural Block 3; **a)** Geometry and frame identification; **b)** Degrees of freedom used for the seismic analysis

5. RESULTS

The seismic analysis was performed with dead load $\mathrm{D} = 0.8\ \mathrm{T/m^2}$ for intermediate floors, and $\mathrm{D} = 0.6\ \mathrm{T/m^2}$ for the roof; likewise the live load is $\mathrm{L} = 0.25\ \mathrm{T/m^2}$ for intermediate floors and $\mathrm{L} = 0.125\ \mathrm{T/m^2}$ for the roof. To determine the seismic effective weights of each floor, 25% of the live load was considered. In Table 3 the total weight at each isolator for the load combination $D + 0.25\ L$ is shown, as well as the effective stiffness found with 3 analytical models and for 3 friction coefficients.

Tabla 3 Effective stiffness using three analytical models and máximum, nominal and mínimum friction coefficients.

ISOLATOR	W (tonf)	MAXIMUM			NOMINAL			MINIMUM		
		Modal-spectral (3 Stages)	Modal-spectral (5 Stages)	ASCE 7-10	Modal-spectral (3 Stages)	Modal-spectral (5 Stages)	ASCE 7-10	Modal-spectral (3 Stages)	Modal-spectral (5 Stages)	ASCE 7-10
F14a	85,6	36,270	39,340	38,850	33,200	35,670	35,264	31,070	33,140	32,794
F13	141,1	59,770	64,830	64,014	54,700	58,780	58,106	51,190	54,600	54,036
F12	55,5	23,490	25,480	25,157	21,500	23,100	22,835	20,120	21,460	21,236
E14a	202,2	85,660	92,910	91,741	78,390	84,240	83,274	73,360	78,250	77,441
E13	333,2	141,130	153,080	151,150	129,150	138,790	137,200	120,870	128,930	127,590
E12	130,8	55,420	60,120	59,361	50,720	54,510	53,883	47,470	50,630	50,109
C14a	228,7	96,860	105,070	103,750	88,650	95,260	94,170	82,960	88,490	87,575
C13	302,0	127,920	138,750	137,010	117,070	125,800	124,360	109,560	116,860	115,650
C12	73,3	31,050	33,680	33,261	28,420	30,540	30,191	26,600	28,370	28,077
A14a	115,5	48,910	53,050	52,386	44,760	48,100	47,551	41,890	44,680	44,221
A13	115,5	48,910	53,050	52,386	44,760	48,100	47,551	41,890	44,680	44,221

Table 3 shows that the 5-stages model has the highest effective stifnesses and that the three-stages model has the lowest values. Furthermore, there is considerable variation between the stiffnesses calculated with the maximum values of the friction coefficient, compared to those found with the nominal and minimum values.

Tabla 4 Damping factors in three anlytical models for máximum, nominal and mínimum friction coefficients.

ISOLATOR	W (tonf)	MAXIMUM			NOMINAL			MINIMUM		
		Modal-Spectral (3 Stages)	Modal-Spectral (5 Stages)	ASCE 7-10	Modal-Spectral (3 Stages)	Modal-Spectral (5 Stages)	ASCE 7-10	Modal-Spectral (3 Stages)	Modal-Spectral (5 Stages)	ASCE 7-10
F14a	85,6	0,2993	0,3256	0,3078	0,2668	0,2925	0,2743	0,2403	0,2652	0,2470
F13	141,1	0,2993	0,3256	0,3078	0,2668	0,2925	0,2743	0,2403	0,2652	0,2470
F12	55,5	0,2993	0,3256	0,3078	0,2668	0,2925	0,2743	0,2403	0,2652	0,2470
E14a	202,2	0,2993	0,3256	0,3078	0,2668	0,2925	0,2743	0,2403	0,2652	0,2470
E13	333,2	0,2993	0,3256	0,3078	0,2668	0,2925	0,2743	0,2403	0,2652	0,2470
E12	130,8	0,2993	0,3256	0,3078	0,2668	0,2925	0,2743	0,2403	0,2652	0,2470
C14a	228,7	0,2993	0,3256	0,3078	0,2668	0,2925	0,2743	0,2403	0,2652	0,2470
C13	302,0	0,2993	0,3256	0,3078	0,2668	0,2925	0,2743	0,2403	0,2652	0,2470
C12	73,3	0,2993	0,3256	0,3078	0,2668	0,2925	0,2743	0,2403	0,2652	0,2470
A14a	115,5	0,2993	0,3256	0,3078	0,2668	0,2925	0,2743	0,2403	0,2652	0,2470
A13	115,5	0,2993	0,3256	0,3078	0,2668	0,2925	0,2743	0,2403	0,2652	0,2470

Table 4 shows the damping factors found with three analytical models. Again the 5-stages model is reporting higher damping factors and the three-stages model gives the lowest values.

Table 5 and Table 6 show the lateral forces and displacements calculated with the three models, respectively. Note that the forces are similar between the 3- and 5- stages models, but they are always higher in the 3-stage model.

Tabla 5 Lateral forces calculated using three analytical models and maximum, nominal and minimum friction coefficients.

BLOCK 3	MAXIMUM			NOMINAL			MINIMUM		
METHOD	**Modal-spectral (3 Stages)**	**Modal-Spectral (5 Stages)**	**ASCE 7-10**	**Modal-Spectral (3 Stages)**	**Modal-Spectral (5 Stages)**	**ASCE 7-10**	**Modal-Spectral (3 Stages)**	**Modal-Spectral (5 Stages)**	**ASCE 7-10**
Isolated	40,4612	37,5946	66,482	40,501	40,476	65,909	31,7868	29,7065	65,735
Story 1	42,2892	38,3212	24,297	42,359	42,318	24,088	30,7979	28,6769	24,024
Story 2	46,1185	43,0132	48,594	45,933	46,106	48,175	32,5204	31,4752	48,048
Story 3	50,0517	44,0163	72,891	49,469	49,966	72,263	29,6751	31,4305	72,072
Story 4	10,3652	6,4248	20,423	10,248	10,349	20,247	4,9011	6,1192	20,194

Tabla 6 Lateral displacements using analytical models and maximum, nominal and minimum friction coefficients.

BLOCK 3	MAXIMUM			NOMINAL			MINIMUM		
METHOD	**Modal-spectral (3 Stages)**	**Modal-Spectral (5 Stages)**	**ASCE 7-10**	**Modal-spectral (3 Stages)**	**Modal-Spectral (5 Stages)**	**ASCE 7-10**	**Modal-spectral (3 Stages)**	**Modal-Spectral (5 Stages)**	**ASCE 7-10**
Isolated	0,3308	0,3508	0,3136	0,3592	0,3361	0,3392	0,4365	0,4097	0,3611
Story 1	0,3509	0,3746	0,3323	0,3792	0,3562	0,3577	0,4593	0,4324	0,3796
Story 2	0,3682	0,3953	0,3501	0,3965	0,3735	0,3754	0,4789	0,4520	0,3972
Story 3	0,3793	0,4088	0,3629	0,4075	0,3846	0,3881	0,4915	0,4646	0,4099
Story 4	0,3607	0,4099	0,3755	0,3880	0,3658	0,4012	0,5008	0,4732	0,4272

In Figure 13 and 14, the displacement and force results are presented for structural block 3 with maximum, minimum and nominal values:

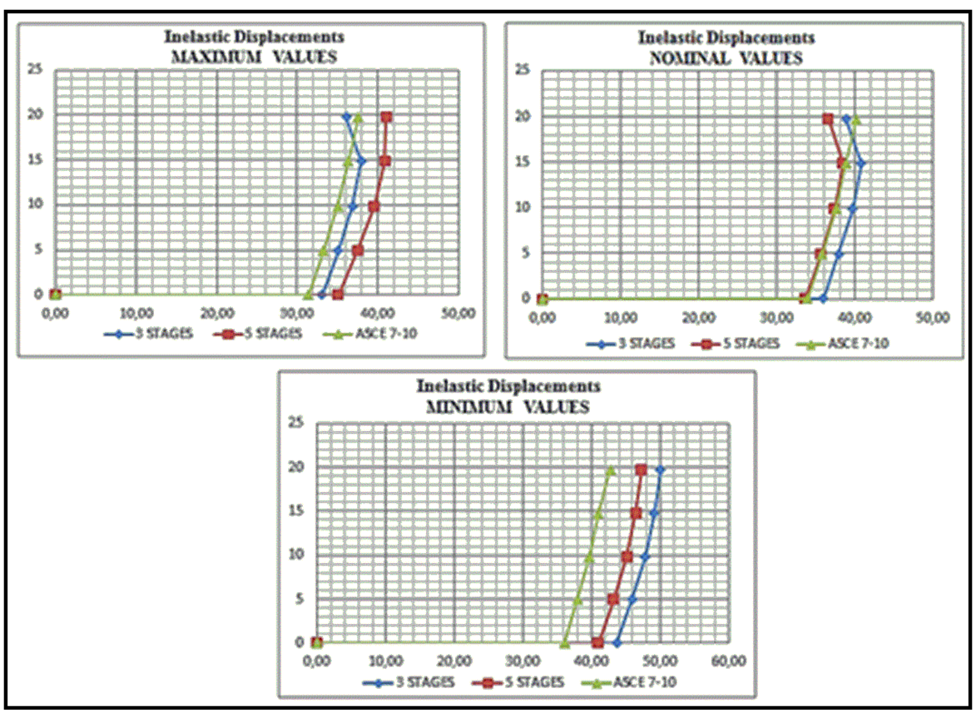

Fig. 13 – Story displacements with maximum, nominal and minimum friction coefficient values

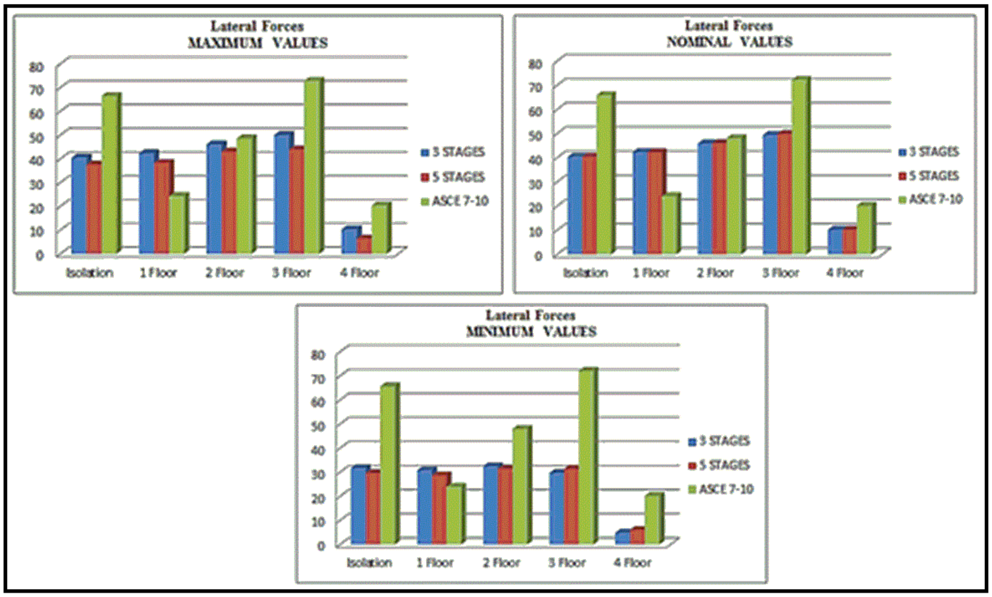

Fig. 14 – Story lateral forces with maximum, nominal and minimum friction coefficient values

6. CONCLUSIONS

At Universidad de las Fuerzas Armadas ESPE in Ecuador, five structural blocks with seismic isolators are being built. The isolation systems were tested to obtain the friction coefficients and other parameters that define the constitutive model relating lateral force vs displacement.

61 isolators were analyzed, with a vertical load of 250 T, each test with three harmonic load cycles with a maximum displacement of 30 cm. The maximum friction coefficient values found for the outer and inner plate are: 0.015672 and 0.068541, respectively. The nominal values are 88.64% and 79.27% of the maximum values and the minimum friction coefficient are 79.86% and 63.07% of the maximum values.

With these values, a seismic analysis was performed on the ESPE structural blocks using the simplified analysis model in ASCE 7, the Mc Vitty and Constantinou (2015) three-stages model and the Fenz and Constantinou (2007) five-stages model.

By working with maximum values of friction coefficient, the lateral forces are greater than those obtained with nominal and minimal friction coefficients, but the difference is around 1%.

Using minimum friction coefficient values, maximum displacements are obtained. In this case, the difference with the other groups of data is around 30%.

On the other hand, the simplified method ASCE 7-10 produced the greatest forces.

Finally, it is important to note that the experimentally found friction coefficients are similar to the maximum, minimum and nominal values given by the manufacturer.

7. REFERENCES

[1] Constantinou M., Aguiar R., Morales E., Caiza P., (2016), "Desempeño de aislador FPT8833/12-12/8-5 en el análisis sísmico del Centro de Investigaciones y de Post Grado de la UFA-ESPE", Revista Internacional de Ingeniería de Estructuras, 21, 1, 1-25.

[2] Fenz, D. M. and Constantinou, M. (2007), Mechanical behavior of multi-spherical sliding bearings, Technical Report MCEER-08-0007, Multidisciplinary Center for Earthquake Engineering Research.

[3] Fenz, D.M. and Constantinou, M.C., (2008), Development, implementation and verification of Dynamic Analysis Models for Multi-Spherical sliding bearings. Report No. MCEER-08-0018, Multidisciplinary Center for Earthquake Engineering Research, Buffalo, NY.

[4] McVitty, W.J. and Constantinou, M.C., (2015), Property modification factors for seismic isolators: Design Guidance for Buildings, Technical Report No. MCEER-15-0005, Multidisciplinary Center for Earthquake Engineering Research, State University of New York at Buffalo, Buffalo, NY, 2015.

[5] Constantinou, M. C, Whittaker, A. S., Kalpakidis, Y., Fenz, D. M. and Warn G. P. (2007), "Performace of Seismic Isolation Hardware under Service and Seismic Loading," Multidisciplinary Center for Earthquake Engineering Research, Technical Report MCEER-07-0012, Buffalo, NY.

[6] EPS (2015), "Production Bearing Test Results for Ecuador University Building (ESPE), Earthquake Protection System, EPS Inc., Mare Island, Vallejo, California.

[7] Aguiar R., (2012), Dinámica de Estructuras con CEINCI-LAB, Instituto Panamericano de Geografía e Historia, IPGH. Segunda edición, 416 p., Quito.

[8] Retamales, R., Bonelli, P., Boroschek, R. y Carvallo, J., (2015), "Aplicación de sistemas de aislación sísmica en edificaciones de mediana altura", XI Congreso Chileno de Sismología e Ingeniería Sísmica, Paper 184, 9 p, Santiago.

[9] Chistopupoulus, C. and Filiatraul, A.(2006). Priciples of passive Suplemental Damping and Seismic Isolation. IUSS Press, Instituto Universitario di Studi Superiori di Pavia, Pavia, Pavia, IT.

[10] Chopra A. K. (2001), Dynamic of structures: Theory and application's to earthquake engineering, 2nd edn. Prentice Hall: Saddle River New York.

[11] ASCE 7-10, Minimum Design Loads for Buildings and Other Structures, American Society of Civil Engineers, 608 p.

[12] Almazán J. L., (2001), Torsión accidental y natural en estructuras aisladas con el sistema de péndulo friccional, Tesis Doctoral. Pontificia Universidad Católica de Chile, 288p., Santiago.

[13] Fenz, D. and Constantinou, M.C. (2006), "Behavior of Double Concave FrictionPendulum Bearing," Earthquake Engineering and Structural Dynamics, Vol. 35,No.11, 1403-1424.

[14] Fadi F., and Constantinou M. (2010), "Evaluation of simplified methods of analysis for structures with triple friction pendulum isolators", Earthquake Engineering and Structural Dynamics, 39, 5-22.

[15] NEC-15 (2015) Norma Ecuatoriana de la Construcción, SE-DS, Cargas Sísmicas. Diseño Sismo Resistente. 138 p. Quito.